



# Pd supported on N-doped-ordered mesoporous carbons' catalysts for selective hydrodechlorination of 4-chlorophenol

Rongrong Li<sup>1</sup> · Shiting Wang<sup>1</sup> · Yuan Hu<sup>1</sup> · Hong Chen<sup>1</sup> · Jingjing Chen<sup>1</sup> · Chu Chu<sup>1</sup> · Jianli Zheng<sup>1</sup>

Received: 18 September 2017 / Accepted: 20 April 2018  
© Institute of Chemistry, Slovak Academy of Sciences 2018

## Abstract

Pd catalysts supported on N-doped-ordered mesoporous carbons (NOMC) have been prepared and tested for selective hydrogenation of 4-chlorophenol (4-CP) with H<sub>2</sub>. The difference from the previous methods is that the NOMC was synthesized using urea as nitrogen source via one-pot route. The rate constant of Pd/NOMC for hydrodechlorination of 4-CP was about 135.9 h<sup>-1</sup> which were higher than Pd/OMC (65.6 h<sup>-1</sup>) and Pd/AC (20.8 h<sup>-1</sup>). It could be attributed to the synergetic effects of mesoporous structure, N-doped supports, and the stabilized small PdNPs. The conversion changed from 100 to 90.2% after the sixth reaction using Pd/NOMC which could be caused by the palladium leaching.

**Keywords** Mesoporous carbon · N-doped · Pd · 4-chlorophenol · Hydrogenation

## Abbreviations

NOMC	N-doped-ordered mesoporous carbons
4-CP	4-Chlorophenol
HDC	Catalytic hydrodechlorination
SAXRD	Small-angle X-ray diffraction
TEM	Transmission electron microscopy
HMT	Hexamethylenetetramine
TMB	1,3,5-Trimethylbenzene
PdNPs	Pd nanoparticles

## Introduction

Chlorophenols are widely used in the production of pesticides, disinfectants, wood preservatives, and personal care formulations (Albers et al. 2001). The residue of these compounds causes a negative effect on the environment and human beings such as the contamination of groundwater due to their acute toxicity and poor biodegradability. Among the current approaches which have been widely employed to

deal with the waste water containing chlorophenols, catalytic hydrodechlorination (HDC) is considered to be an environmental friendly one by the breaking up of the C–Cl bond and thus transforming toxic substances into safe compounds or even useful materials (Molina et al. 2014). In general, the catalytic HDC is conducted under a reduction atmosphere of molecular hydrogen and by contacting with supported metallic catalysts such as Pd (Aramendia et al. 1999; Baeza et al. 2016; Benitez and Gloria 2000; Bernard et al. 1993; Calvo et al. 2009), Pt (Chang et al. 2016; Datta et al. 2010), and Rh (Díaz et al. 2010, 2011, 2016 Gómez-Quero et al. 2011). Pd has been proven to be the most promising one because of its high activity in such degradation of chlorophenols at ambient conditions. Nevertheless, severe catalyst deactivation originated due to formation of strong bond between Cl and Pd (Gómez-Quero et al. 2010a, b), aggregation of Pd nanoparticles (Gong et al. 2013; Hashimoto and Ayame 2003), and/or carbonaceous deposited on Pd particles (Hildebrand et al. 2009; Huang et al. 2008; Jadbabaei et al. 2017).

Based on the above, there remains as a challenge to find stable catalysts for selective hydrogenation of chlorophenols. Therefore, activated carbon, pillared clays (Molina et al. 2014),  $\gamma$ -Al<sub>2</sub>O<sub>3</sub> (Munoz et al. 2014), and silica (Bovkun et al. 2005; Li et al. 2009, 2012, 2017; Liu et al. 2010, 2011, 2012; Lyonnard et al. 2002) were used as supports for HDC, and the phenol is further converted into cyclohexanol. The research of carbon carrier is the most widespread since its high adsorption capacity, excellent dynamic behavior, and high resistance to abrasion (Böhringer et al. 2011;

**Electronic supplementary material** The online version of this article (<https://doi.org/10.1007/s11696-018-0477-8>) contains supplementary material, which is available to authorized users.

✉ Rongrong Li  
lrr@tzc.edu.cn

<sup>1</sup> School of Pharmaceutical and Chemical Engineering, TaiZhou University, Taizhou 318000, Zhejiang, People's Republic of China

Romero-Anaya et al. 2014). In last several years, functionalized mesoporous superfluos have attracted an intense interest due to their higher surface areas, structural regularity, and regulable pore size (Mitoma et al. 2009). Particularly, the  $\text{NH}_2$  groups on the surface of the materials are beneficial to improve the activity and stability, since the metal nanoparticles anchored and well dispersed (Molina et al. 2010). N-doped-ordered carbon matrixes, which could change the physicochemical properties of the materials, have been used as supports to synthesize supported nanoparticle catalysts for hydrogenation (Moon et al. 1998; Öcal et al. 1999; Osegueda et al. 2015; Rong et al. 2013), oxidation (Santiago et al. 2008), and coupling reaction (Shao et al. 2010). However, the application of metal nanoparticles dispersed on the N-doped OMC supports for the HDC reaction is rare.

In last several years, an organic–organic co-assembly synthesis method was proved as a credible method to synthesize OMC by either hydrothermal (Sohn et al. 2017; Vinu et al. 2005; Wang et al. 2014) or an evaporation-induced self-assembly procedure (Wang et al. 2011; Wiersma et al. 1996, 2001; Xue et al. 2008). Therefore, the aim of the current study is to obtain N-doped OMC by one-pot route synthesis and used urea as the nitrogen source. The direct synthesized NOMC could be favorable in practical applications, which can keep the high-ordered mesoporous structures unchanged and modulate the N content easily. The as-prepared NOMC was used support for immobilization of Pd catalyst during the HDC of 4-chlorophenol in aqueous solution using direct hydrogen. The activity of catalysts was checked in the batch mode which was used to evaluate the effects of reaction temperature and metal loading with 4-CP as target compound. The effect of the N content of NOMC in the preparation of the catalysts has been studied.

## Methods

### Catalyst preparation

Triblock poly (ethylene oxide)-*b*-poly (propylene oxide)-*b*-poly (ethylene oxide) copolymers Pluronic F127 (EO106 PO70 EO106,  $M_{\text{av}} = 12600$ ) were purchased from Sigma-Aldrich Corp. Other chemicals were purchased from Sinopharm Chemical Reagent Corp. All chemicals were used as received without further treatment.

### Synthesis of NOMC

In a typical procedure, About 3.2 g urea, 1.10 g of resorcinol, 0.70 g of hexamethylenetetramine (HMT), 2.00 g of Pluronic F127, 0.40 g of 1,3,5-trimethylbenzene (TMB), 52 mL of deionized water, and 2.00 mL of aqueous ammonia (28 wt%) were mixed in random sequence. After stirring at

room temperature for 1 h, the resultant dark green solution was further stirred in a water-bath under reflux condenser at 80 °C. Green precipitation was observed after about 20 min. After continuously stirring for another 24 h, the black solid products were collected by sedimentation separation, filtration, washed with water, and air-dried at room temperature. Finally, the as-made composite (NOMC) was thermally treated at 900 °C for 3 h, with a heating rate of 1 °C  $\text{min}^{-1}$  under a nitrogen atmosphere, to obtain the NOMC. The synthesis of OMC was also carried out through the Lieu et al. method (Lyonnard et al. 2002) for comparison with other catalysts.

### Immobilization of Pd nanoparticles

The corresponding PdNP catalysts Pd/NOMC synthesized via improved synthetic method reported by Li et al. (2017).

### Characterization techniques

The microstructure and component analysis of the alloy NPs was examined by transmission electron microscopy (TEM) equipped with high-angle annular dark-field (HAADF) attachment and energy-dispersive X-ray spectroscopy (EDX) (Philips-FEI Tecnai G2 F30 S-Twin). The TEM samples were prepared by dispersing the powder products in pure ethanol using ultrasonic cleaner at room temperature for 0.5 h and transferring them to carbon-coated copper grids. Average particle sizes were determined by measuring at least 100 particles for each sample analyzed, from at least five different micrographs. X-ray diffraction measurements of the catalyst samples were performed on a PANalytical-X'Pert PRO generator with  $\text{Cu K}\alpha$  radiation ( $\lambda = 0.1541$  nm). X-ray fluorescence by dispersive energy (XRF) was acquired using a Thermo ARLADVANT'X IntelliPower TM 4200 spectrometer. The samples were excited with the Rh X-ray tube operated at 40 kV and 1.25 mA. X-ray photoelectron spectroscopy (XPS) was acquired with a Kratos AXIS Ultra DLD spectrometer. XPS analysis was performed using the monochromatized aluminum X-ray source and pass energy of the electron analyzer of 40 eV. The pressure in the sample analysis chamber was lower than  $6 \times 10^{-9}$  Torr during data acquisition. Binding energies (BE) were referred to the C1 s line at 284.8 eV.

### Catalysis tests

Catalytic tests were conducted in a 50 mL Schlenk glass batch reactor with a magnetic bar; 0.025 g Pd/NOMC catalyst, 5 mL ( $1.5 \text{ g L}^{-1}$ ) 4-CP, and 25 mL deionized water were introduced into the glass reactor, and then, it was vacuumed and purged with  $\text{H}_2$  three times before it was finally pressurized with 1.0 atm of  $\text{H}_2$  gas. Subsequently, the reaction mixture was

stirred at 303 K and the stirring rate is 1000 rpm. After cooling to RT, excess H<sub>2</sub> was carefully released, and the internal standard (ethylene glycol) was added. 4-CP, phenol, cyclohexanone, and cyclohexanol were analyzed by a gas chromatograph (GC 2010plus, Shimadzu). The temperatures of the injection port and the flame ionization detector were 280 °C. Samples were injected in the splitless mode onto a 25 m length × 0.32 mm i.d. capillary column (CP-FFAP CB, Varian). The following temperature program: the initial temperature of the column was 60 °C, held for 1 min, and the rate of the temperature increase was 20 °C min<sup>-1</sup> up to 280 °C, with a final hold time of 2 min. The carrier gas was nitrogen; meanwhile, hydrogen and oxygen were fed to the FID. All the gas has a purity of 99.999%. The reaction fluid is filtered through an inorganic membrane material to prevent the catalyst from entering gas chromatography. The relative peak area % was converted to mass% using regression equations based on detailed calibration plots. Preliminary control 4-CP HDC experiments with NOMC were carried out to check any potential interaction between 4-CP, H<sub>2</sub> and NOMC in the absence of catalysts. No effect of NOMC was observed and no reaction products were detected in the absence of catalyst. Different stirring velocities were also checked, confirming that the process takes place under chemical control. The rate of 4-CP disappearance was calculated from a pseudo-first-order equation:

$$(-r_{4\text{-cp}}) = \frac{-dC_{4\text{-cp}}}{dt} = k_1 \times C_{4\text{-cp}}$$

$$t = 0; \quad C_{4\text{-cp}} = C_0.$$

The concentration of hydrogen can be included in the pseudo-first-order rate constant ( $k_1$ ), since hydrogen is in great excess.

The effluent was analyzed and three analyses were made at each temperature. The conversion of 4-CP ( $X_{\text{CP}}$ ) is defined by the following:

$$X_{\text{CP}} = \frac{[\text{CP}]_0 - [\text{CP}]}{[\text{CP}]_0} \times 100\%.$$

The selectivity with respect to phenol (e.g.) is given as the mass% phenol ( $m_{\text{phenol}}\%$ ) in the terms of the total mass of products formed, and was calculated using the following equations:

$$S_{\text{phenol}} = \frac{m_{\text{phenol}}\%}{m_{\text{cyclohexanol}}\% + m_{\text{cyclohexanone}}\% + m_{\text{phenol}}\%} \times 100\%,$$

$$S_{\text{cyclohexanol}} = \frac{m_{\text{phenol}}\%}{m_{\text{cyclohexanol}}\% + m_{\text{cyclohexanone}}\% + m_{\text{phenol}}\%} \times 100\%,$$

$$S_{\text{cyclohexanone}} = \frac{m_{\text{phenol}}\%}{m_{\text{cyclohexanol}}\% + m_{\text{cyclohexanone}}\% + m_{\text{phenol}}\%} \times 100\%,$$

where  $m_{\text{cyclohexanol}}\%$ ,  $m_{\text{cyclohexanone}}\%$ , and  $m_{\text{phenol}}\%$  represent the mass fraction of cyclohexanol, cyclohexanone, and phenol in the mixture.

## Results and discussion

### Characterization of the catalyst

N<sub>2</sub> adsorption–desorption isotherms of NOMC have an obvious condensation step at  $P/P^0 = 0.4\text{--}0.6$ , which can be indexed as typical type-IV curves and showing a uniform mesopore (Fig. 1). The isotherms do not fit well H1-type hysteresis loop, since the mesopore may have some block in pore canals. The BET surface area, pore volume, and pore size are listed in Table S1. After adding urea, the  $S_{\text{BET}}$  values are lower than that of the reported OMCs (870 m<sup>2</sup> g<sup>-1</sup> for RF-1-900 and 853 m<sup>2</sup> g<sup>-1</sup> for RF-2-900) (Mitoma et al. 2009) which might be attributed to N-doping reaction by decomposition of urea into radicals like ·NH<sub>2</sub> and ·NH. These reactions could result in the porosity change (Xia et al. 2009). The surface area and pore volume of PdNPs supported NOMC and NOMC are changed slightly after the supporting PdNPs, suggesting that the ordered mesopores are still well preserved after doping by amino functional groups and the mesostructure is not blocked by Pd nanoparticles. Small-angle X-ray diffraction (SAXRD) characterization in Fig. 2a could also prove this result.

In Fig. 2a, the SAXRD of NOMC without addition of TMB shows one weak peak that can be indexed as (110) reflections of the body-centered cubic Imm symmetry. Figure 2 shows the SAXRD of NOMC, which shows that one resolved peak can be indexed as p6m space group with 2D hexagonal structure (Mitoma et al. 2009). Compared to the

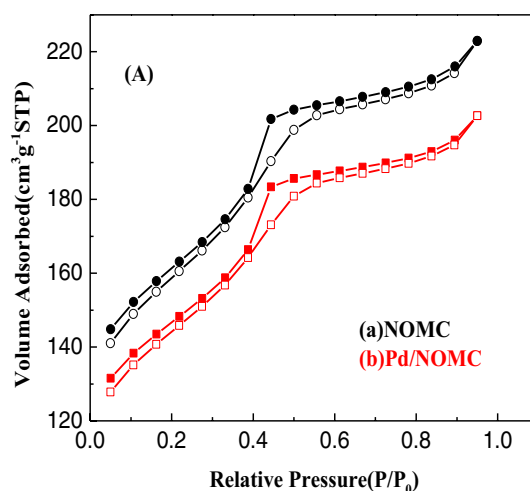
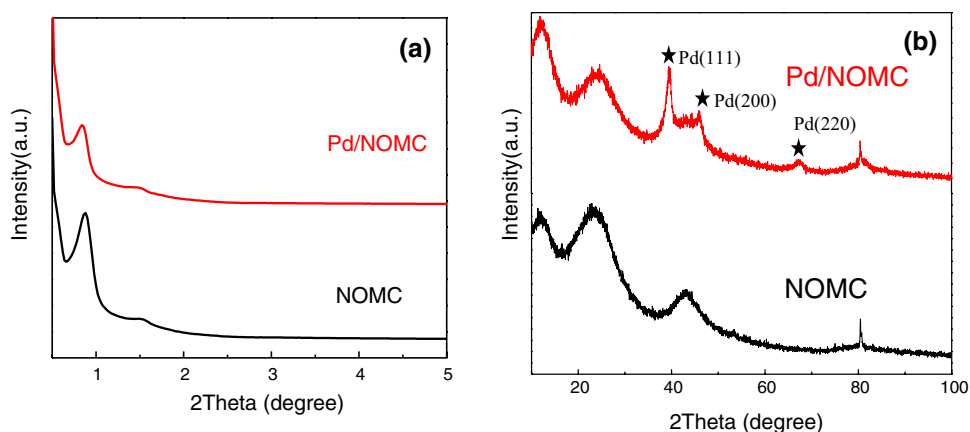


Fig. 1 N<sub>2</sub> sorption isotherms of NOMC and Pd@NOMC

**Fig. 2** SAXRD (a) and WAXRD (b) patterns of NOMC and Pd/NOMC



reported OMCs, the diffraction intensity decreases slightly after doping by N groups, which indicates that the ordered mesostructures are slightly changed. Wide-angle XRD patterns of NOMC show that nanoparticles are well dispersed and high-intensity 002 and 100 diffractions belong to graphitic carbon. The patterns of Pd and Pd/NOMC-T in Fig. 2b show Pd (111), Pd (200), and Pd (220) diffractions which are observed obviously, which illustrate that the extra small Pd nanoparticles are well dispersed on the surface of the N-doped OMC matrix.

The structure of the Pd/NOMC was examined by transmission electron microscopy (TEM) (Fig. 3). The TEM images show that the sample has high ordered of periodicity viewed from the [110] direction; this result also illustrates that these NOMC still maintain mesostructure and not blocked by PdNPs. The distribution of particle size image of Pd/NOMC is showed in Fig. S1. The PdNPs' average size is

approximately 3.4 nm which are homogeneously dispersed on the surface of the NOMC. All the PdNPs are uniform and no obvious agglomeration is detected in the HAADF-STEM images. Moreover, the N-doped-ordered mesoporous canals are arranged in regular intervals, which may indicate that the structures are no degenerated after the immobilization of metal NPs. The well-dispersed PdNPs could also attribute to N-hybrids which promote the stabilization of metal NPs.

XPS results are listed in Table S1, Fig. S2, and Fig. 4. The carbon, oxygen, and nitrogen elements have strong signals. The nitrogen content of Pd/NOMC is 1.73 wt%. The C 1s spectra of Pd/NOMC are showed in Fig. S2, which could be attributed to C–C (284.8 eV), C–O (285.3 eV), C=O (286.6 eV), and C=O–C (289.6 eV). The N1s XP spectrum of Pd/NOMC showed in Fig. 4 might be well identified to four components (Xia et al. 2004; Xu et al. 2012; Shao et al. 2011), which could be attributed to pyridinic-N (398.4 eV),

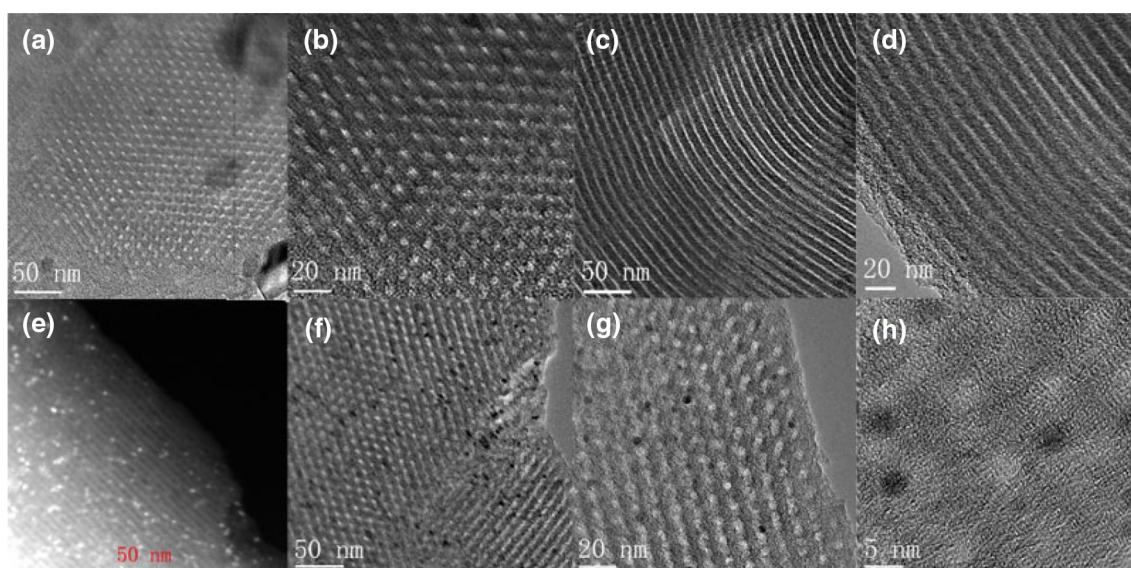


**Fig. 3** STEM images of NOMC (a–d) and Pd/NOMC (e–h)

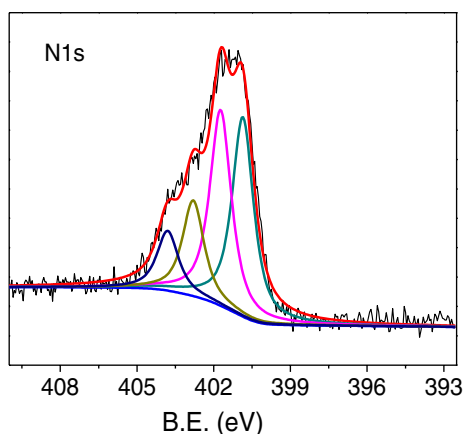


Fig. 4 XPS spectra N 1s spectra of Pd/NOMC

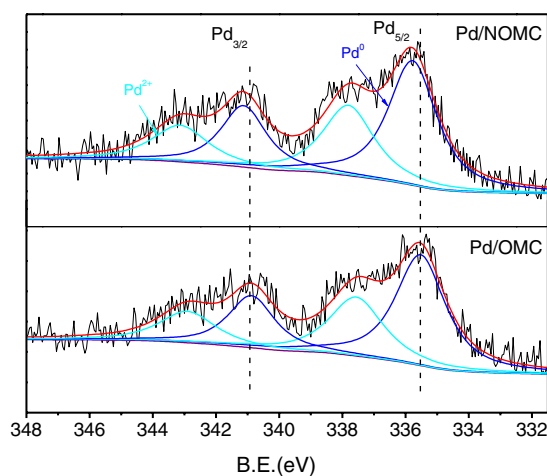


Fig. 5 XPS spectra of Pd 3d spectra of Pd/NOMC and Pd/OMC

pyrrolic-N (399.7 eV), graphitic-N (401.2 eV), and nitrogen-oxides (404.4 eV). The XPS spectra of Pd 3d peaks (Fig. 5) have a doublet attributed to Pd 3d<sub>5/2</sub> and 3d<sub>3/2</sub>. The Pd 3d<sub>5/2</sub> peak at 335.8 eV is related to Pd<sup>0</sup>, while the Pd

3d<sub>3/2</sub> peak at 337.8 eV is related to Pd<sup>2+</sup>. XPS results have a positive shift of ca. 0.3 eV comparing with the Pd/OMC case in our early work (Baeza et al. 2016). Shao et al. (2011) compared the supported Pd catalysts on ordered mesoporous carbon (OMC) and activated carbon (AC) for the liquid-phase catalytic hydrodechlorination (HDC) of 2,4-dichlorophenol. In comparison with Pd/AC, Pd particles of Pd/OMC were effectively confined in the mesopores of OMC, resulting in high Pd dispersion and Pd<sup>2+</sup> content. Gómez-Sainero et al. (2002) studied the catalytic HDC of CCl<sub>4</sub> over Pd/AC and concluded that the coexistence of Pd<sup>2+</sup> and Pd<sup>0</sup> was essential for the effective HDC of CCl<sub>4</sub>, wherein Pd<sup>0</sup> acted as the active site for H<sub>2</sub> activation and Pd<sup>2+</sup> served as the active site for the activation of C–Cl bond via abstraction of nucleophilic chloride anion and formation of highly reactive +CCl<sub>3</sub> ion. Hence, at similar reduction temperature, the higher catalytic activity of Pd/OMC can be attributed to its higher Pd<sup>2+</sup> content. It is well accepted that the direction of the core-level shift is consistent with that of the valence band shift, which could also be attributed to the partial electron transfer from N to Pd atoms. This likely arises from the electron transfer between metal Pd and NOMC which makes Pd electron-deficient. The latter suggests a strong interaction between Pd NPs and the substitutional nitrogen defect sites (Baeza et al. 2016; Benitez and Gloria 2000; Bernard et al. 1993).

### Hydrodechlorination of 4-CP

The catalyst Pd/NOMC was used for the selective hydrogenation of 4-chlorophenol, and the results are shown in Table 1. Selectivity of 4-CP dehydrochlorination to phenol was decreased from 100 to 75% and the product of cyclohexanone and cyclohexanol was increased. While the conversion of 4-CP was only 15.3 or 48.3% over Pd/AC or Pd/OMC prepared by a similar method. Selectivity of 4-CP dehydrochlorination to cyclohexanone was about 18.5% which was much lower than Pd/OMC (1.2%) and Pd/C (0.8%). More cyclohexanone will be getting by deep hydrogenation which

**Table 1** Catalytic performance of different catalyst for hydrodechlorination of 4-CP

Entry	Catalyst	Pd (mg kg <sup>-1</sup> ) analyzed by of ICP		Conversion (%)	Selectivity (%)		
		Fresh	Used		Cyclohexanol	Cyclohexanone	Phenol
1	NOMC	–	–	0	0	0	0
2	Pd/C <sup>a</sup>	905	705	15.3	0	0.8	99.2
3	Pd/OMC <sup>a</sup>	895	783	48.3	0	1.2	98.8
4	Pd/NOMC <sup>a</sup>	911	873	100	5.8	18.5	75.7

The conversion and selectivity was determined by GC. Reaction conditions: 0.025 g catalyst; 5 mL (1.5 g L<sup>-1</sup>) 4-CP, 25 mL H<sub>2</sub>O, time=1.5 h, P (H<sub>2</sub>)=1.0 atm, temperature=303 K, and stirring rate=1000 rpm

<sup>a</sup>Pd loading wt%=1%

may be attributed to the higher active site for phenol species in Pd/NOMC. During the HDC process, the chemistry of the support plays a key role on the performance of the catalysts, especially in their deactivation behavior through the metal/support interactions and reactant/support interactions (Li et al. 2013; Yoneda et al. 2007). Yuan and Keane (2004a, 2007) suggested that the catalyst activity can be reestablished due to migration of halide ions from the surface of the metal to the support to form halogenated species, thus inhibiting the gradual deactivation of catalyst. Moreover, it was proposed that the larger particle size (ca. 4 nm) of the active site of the catalyst exhibited a stronger resistance for the passivation of the catalyst (Yuan and Keane 2004b; Zhang et al. 2006, 2011). Zhang et al. (2013) studied HDC of 4-CP in aqueous solution with formic acid using a Pd/AC. Conversion values above 99% for 4-CP were obtained and the highest selectivity of 4-CP dehydrochlorination to cyclohexanone was 12% at 348 K. A gradual loss of activity was observed in successive runs when using Pd-Al pillared clays as catalysts for the HDC (Molina et al. 2018). The conversion of 4-CP was about 100% on reduced graphene oxide, but the temperature was 317 K (Deng et al. 2014). In our study, we can get the same selectivity at 306 K.

In this work, besides the possible reasons mentioned above, the remained nitrogen functional groups of NOMC could avoid the leaching and the agglomeration of Pd nanoparticles. In addition, the support without the doping of nitrogen was not used as a controllable support to investigate the effect of the N-doping. The conversion and product selectivities are given in Fig. S3; the recycling of the catalyst Pd/NOMC for HDC is added in Fig. S4, Supporting Information.

## Conclusions

Using urea as a nitrogen source and resorcinol/hexamethylenetetramine as a carbon source, nitrogen-doped OMC has been successfully synthesized by a self-assembly process with Pluronic F127 in aqueous solutions. Pd catalysts supported on NOMC have been prepared and tested for selective hydrogenation of 4-CP with H<sub>2</sub>. The mesoporous structure is still well arranged in regular intervals after the N-doped and immobilization of metal NPs, which could indicate that the N-doped-ordered mesochannels is stable. The rate constant of Pd/NOMC for hydrodechlorination of 4-CP was about 135.9 h<sup>-1</sup> which were higher than Pd/OMC (65.6 h<sup>-1</sup>) and Pd/AC (20.8 h<sup>-1</sup>). The doped nitrogen was found not only to disperse and stabilize the ultrasmall particle size of Pd but also to promote the catalytic hydrogenation performance. The conversion changed from 100 to 90.2% after the six reaction using Pd/NOMC which could be caused by the palladium leaching (from 911 to 873 mg kg<sup>-1</sup>).

**Acknowledgements** The project was supported by the National Natural Science Foundation, China (21506138), and the Natural Science Foundation of Zhejiang Province, China (LQ15B060001).

## References

- Albers P, Pietsch J, Parker S (2001) Poisoning and deactivation of palladium catalysts. *J Mol Catal A Chem* 173:275–286
- Aramendia M, Borau V, Garcia I, Jimenez C, Lafont F, Marinas A, Marinas J, Urbano F (1999) Influence of the reaction conditions and catalytic properties on the liquid-phase hydrodechlorination of chlorobenzene over palladium-supported catalysts: activity and deactivation. *J Catal* 187:392–399
- Baeza J, Calvo L, Rodriguez J, Gilarranz M (2016) Catalysts based on large size-controlled Pd nanoparticles for aqueous-phase hydrodechlorination. *Chem Eng J* 294:40–48
- Benitez J, Gloria D (2000) Effect of chlorine released during hydrodechlorination of chlorobenzene over Pd, Pt and Rh supported catalysts. *React Kinet Catal Lett* 70:67–72
- Bernard C, Marie C, Francois F, Didier T (1993) Conversion under hydrogen of dichlorodifluoromethane over supported palladium catalysts. *J Catal* 141:21–33
- Böhringer B, Guerra Gonzalez O, Eckle I, Müller M, Giebelhausen J, Schrage C, Fichtner S (2011) Polymer-based spherical activated carbons-from adsorptive properties to filter performance. *Chem Ing Tech* 83:53–60
- Bovkun TT, Sasson Y, Blum J (2005) Conversion of chlorophenols into cyclohexane by a recyclable Pd-Rh catalyst. *J Mol Catal A Chem* 242:68–73
- Calvol L, Gilarranz M, Casas J, Mohedano A, Rodriguez J (2009) Hydrodechlorination of 4-chlorophenol in water with formic acid using a Pd/activated carbon catalyst. *J Hazard Mater* 161:842–847
- Chang W, Kim H, Lee G, Byoung J (2016) Catalytic hydrodechlorination reaction of chlorophenols by Pd nanoparticles supported on graphene research on chemical intermediates. *Res Chem Intermed* 42:71–82
- Datta K, Reddy K, Ariga K, Vinu A (2010) Gold nanoparticles embedded in a mesoporous carbon nitride stabilizer for highly efficient three-component coupling reaction. *Angew Chem* 49:5961–5965
- Deng H, Fan G, Wang C, Zhang L (2014) Aqueous phase catalytic hydrodechlorination of 4-chlorophenol over palladium deposited on reduced graphene oxide. *Catal Commun* 46:219–223
- Diaz E, Ordóñez S, Bueres R, Asedegbega-Nieto E, Sastre H (2010) High-surface area graphites as supports for hydrodechlorination catalysts: tuning support surface chemistry for an optimal performance. *Appl Catal B Environ* 99:181–190
- Diaz E, Mohedano A, Casas J, Calvo J, Gilarranz M, Rodriguez J (2011) Comparison of activated carbon-supported Pd and Rh catalysts for aqueous-phase hydrodechlorination. *Appl Catal B Environ* 106:469–475
- Diaz E, Mohedano A, Casas J, Rodriguez J (2016) Analysis of the deactivation of Pd, Pt and Rh on activated carbon catalysts in the hydrodechlorination of the MCPA herbicide. *Appl Catal B Environ* 181:429–435
- Gómez-Quero S, Díaz E, Cárdenas-Lizana F, Keane M (2010a) Solvent effects in the catalytic hydrotreatment of haloaromatics over Pd/Al<sub>2</sub>O<sub>3</sub> in water + organic mixtures. *Chem Eng Sci* 65:3786–3797
- Gómez-Quero SF, Cárdenas-Lizana F, Keane MA (2010b) Solvent effects in the hydrodechlorination of 2,4-dichlorophenol over Pd/Al<sub>2</sub>O<sub>3</sub>. *AIChE J* 56:756–767
- Gómez-Quero S, Cárdenas-Lizana F, Keane M (2011) Liquid phase catalytic hydrodechlorination of 2,4-dichlorophenol over Pd/Al<sub>2</sub>O<sub>3</sub>: batch vs. continuous operation. *Chem Eng J* 166:1044–1051

- Gómez-Sainero LM, Seoane XL, Fierro JLG, Arcoya A (2002) Liquid-phase hydrodechlorination of  $\text{CCl}_4$  to  $\text{CHCl}_3$  on Pd/carbon catalysts: nature and role of Pd active species. *J Catal* 209:279–288
- Gong Y, Zhang P, Xu X, Li Y, Li H, Wang Y (2013) A novel catalyst Pd@omp-g- $\text{C}_3\text{N}_4$  for highly chemoselective hydrogenation of quinoline under mild conditions. *J Catal* 297:272–280
- Hashimoto Y, Ayame A (2003) Low-temperature hydrodechlorination of chlorobenzenes on platinum-supported alumina catalysts. *Appl Catal A Gen* 250:247–254
- Hildebrand H, Mackenzie K, Kopinke F-D (2009) Highly active Pd-on-magnetite nanocatalysts for aqueous phase hydrodechlorination reactions. *Energy Environ Sci* 43:3254–3259
- Huang Y, Cai H, Feng D, Gu D, Deng Y, Tu B, Wang H, Webley P, Zhao D (2008) One-step hydrothermal synthesis of ordered mesostructured carbonaceous monoliths with hierarchical porosities. *Chem Commun* 23:2641–2643
- Jadababaei N, Ye T, Shuai D, Zhang H (2017) Development of palladium-resin composites for catalytic hydrodechlorination of 4-chlorophenol. *Appl Catal B Environ* 205:576–586
- Li X, Wang H, Robinson J, Sanchez H, Diankov G, Dai H (2009) Simultaneous nitrogen doping and reduction of graphene oxide. *Am Chem Soc* 131:15939–15944
- Li X, Wang X, Markus A (2012) Mesoporous g- $\text{C}_3\text{N}_4$  nanorods as multifunctional supports of ultrafine metal nanoparticles: hydrogen generation from water and reduction of nitrophenol with tandem catalysis in one step. *Chem Sci* 3:2170–2174
- Li Y, Xu X, Zhang P, Wang Y (2013) Highly selective Pd@mpg- $\text{C}_3\text{N}_4$  catalyst for phenol hydrogenation in aqueous phase. *RSC Adv* 27:10973–10982
- Li R, Zhao J, Han D, Li X (2017) One-step synthesis of B-doped mesoporous carbon as supports of Pd nanoparticles for liquid phase catalytic hydrodechlorination. *Catal Commun* 97:116–119
- Liu L, Wang F, Shao G, Yuan Z (2010) A low-temperature autoclaving route to synthesize monolithic carbon materials with an ordered mesostructure. *Carbon* 48:2089–2099
- Liu D, Lei J, Guo L, Deng K (2011) Simple hydrothermal synthesis of ordered mesoporous carbons from resorcinol and hexamine. *Carbon* 49:2113–2119
- Liu D, Lei J, Guo L, Qu D, Li Y, Su B (2012) One-pot aqueous route to synthesize highly ordered cubic and hexagonal mesoporous carbons from resorcinol and hexamine. *Carbon* 50:476–487
- Lyonnard S, Bartlett J, Sizgek E, Finnie K, Zemb T, Woolfrey J (2002) Role of interparticle potential in controlling the morphology of spray-dried powders from aqueous nanoparticle sols. *Langmuir* 18:10386–10397
- Mitoma Y, Kakeda M, Simion A, Egashira N, Simion C (2009) Metallic Ca-Rh/C-methanol, a high-performing system for the hydrodechlorination/ring reduction of mono- and poly chlorinated aromatic substrates. *Energy Environ Sci* 43:5952–5958
- Molina C, Pizarro A, Gilarranz M, Casas J, Rodriguez J (2010) Hydrodechlorination of 4-chlorophenol in water using Rh-Al pillared clays. *Chem Eng J* 160:578–585
- Molina CB, Pizarro AH, Casas JA, Rodriguez JJ (2014) Aqueous-phase hydrodechlorination of chlorophenols with pillared clays-supported Pt, Pd and Rh catalysts. *Appl Catal B Environ* 148:330–338
- Molina CB, Calvo L, Gilarranz MA, Casas JA, Rodriguez JJ (2009) Pd-Al pillared clays as catalysts for the hydrodechlorination of 4-chlorophenol in aqueous phase. *J Hazard Mater* 172:214–223
- Moon D, Jo Chung M, You Park K, In Hong S (1998) Deactivation of Pd catalysts in the hydrodechlorination of chloropentafluoroethane. *Appl Catal A Gen* 168:159–170
- Munoz M, de Pedro ZM, Casas JA, Rodriguez JJ (2014) Combining efficiently catalytic hydrodechlorination and wet peroxide oxidation (HDC-CWPO) for the abatement of organochlorinated water pollutants. *Appl Catal A* 488:78–85
- Öcal M, Maciejewski M, Baiker A (1999) Conversion of  $\text{CCl}_2\text{F}_2$  (CFC-12) in the presence and absence of  $\text{H}_2$  on sol-gel derived Pd/ $\text{Al}_2\text{O}_3$  catalysts. *Appl Catal B Environ* 21:279–289
- Osegueda O, Dafinov A, Llorca J, Medina F, Sueiras J (2015) Heterogeneous catalytic oxidation of phenol by in situ generated hydrogen peroxide applying novel catalytic membrane reactors. *Chem Eng J* 262:344–355
- Romero-Anaya AJ, Ouzzine M, Lillo-Ródenas MA, Linares-Solano A (2014) *Carbon* 68:296–307
- Rong H, Cai S, Niu Z, Li Y (2013) Composition-dependent catalytic activity of bimetallic nanocrystals: AgPd-catalyzed hydrodechlorination of 4-chlorophenol. *ACS Catal* 3:1560–1563
- Santiago G, Fernando C, Mark K (2008) Effect of metal dispersion on the liquid-phase hydrodechlorination of 2,4-dichlorophenol over Pd/ $\text{Al}_2\text{O}_3$ . *Ind Eng Chem Res* 47:6841–6853
- Shao Y, Xu Z, Wan H, Chen H, Liu F, Li L, Zheng S (2010) Influence of  $\text{ZrO}_2$  properties on catalytic hydrodechlorination of chlorobenzene over Pd/ $\text{ZrO}_2$  catalysts. *J Hazard Mater* 179:135–140
- Shao Y, Xu Z, Wan H, Wan Y, Chen H, Zheng S, Zhu D (2011) Enhanced liquid phase catalytic hydrodechlorination of 2,4-dichlorophenol over mesoporous carbon supported Pd catalysts. *Catal Commun* 12:1405–1409
- Sohn H, Celik G, Gunduz S, Majumdar SS, Dean SL, Edmiston PL, Ozkan US (2017) Effect of high-temperature on the swellable organically-modified silica (SOMS) and its application to gas-phase hydrodechlorination of trichloroethylene. *Appl Catal B Environ* 209:80–90
- Vinu A, Ariga K, Mori T, Nakanishi T, Hishita S, Golberg D, Bando Y (2005) Preparation and characterization of well-ordered hexagonal mesoporous carbon nitride & dagger. *Adv Mater* 17:1648–1652
- Wang Y, Yao J, Li H, Su D, Markus A (2011) Highly selective hydrogenation of Phenol and derivatives over a Pd@Carbon nitride catalyst in aqueous media. *J Am Chem Soc* 133:2362–2365
- Wang J, Liu H, Gu X, Wang H, Su D (2014) Synthesis of nitrogen-containing ordered mesoporous carbon as a metal-free catalyst for selective oxidation of ethylbenzene. *Chem Commun* 50:9182–9184
- Wiersma A, Van de Sandt E, Makkee M, Luteijn C, Van Bekkum H, Moulijn JA (1996) Process for the selective hydrogenolysis of  $\text{CCl}_2\text{F}_2$  (CFC-12) into  $\text{CH}_2\text{F}_2$  (HFC-32). *Catal Today* 27:257–264
- Wiersma A, van de Sandt E, Makkee M, Moulijn JA (2001) Deactivation of palladium on activated carbon in the selective hydrogenolysis of  $\text{CCl}_2\text{F}_2$  (CFC-12) into  $\text{CH}_2\text{F}_2$  (HFC-32). *Appl Catal A Gen* 212:223–238
- Xia C, Xu J, Wu W, Liang X (2004) Pd/C-catalyzed hydrodehalogenation of aromatic halides in aqueous solutions at room temperature under normal pressure. *Catal Commun* 5:383–386
- Xia C, Liu Y, Zhou S, Yang C, Liu S, Xu J, Yu J, Chen J, Liang X (2009) The Pd-catalyzed hydrodechlorination of chlorophenols in aqueous solutions under mild conditions: a promising approach to practical use in wastewater. *J Hazard Mater* 169:1029–1033
- Xu X, Li Y, Gong Y, Zhang P, Li H, Wang Y (2012) Synthesis of palladium nanoparticles supported on mesoporous N-doped carbon and their catalytic ability for biofuel upgrade. *J Am Chem Soc* 134:16987–16990
- Xue C, Tu B, Zhao D (2008) Evaporation-induced coating and self-assembly of ordered mesoporous carbon-silica composite monoliths with macroporous architecture on polyurethane foams. *Adv Funct Mater* 18:3914–3921
- Yoneda T, Takido T, Konuma K (2007) Hydrodechlorination reactivity of para-substituted chlorobenzenes over platinum/carbon catalyst. *J Mol Catal A Chem* 265:80–89
- Yuan G, Keane M (2004a) Liquid phase hydrodechlorination of chlorophenols over Pd/C and Pd/ $\text{Al}_2\text{O}_3$ : a consideration of HCl/catalyst interactions and solution pH effects. *Appl Catal B Environ* 52:301–314

- Yuan G, Keane M (2004b) Role of base addition in the liquid-phase hydrodechlorination of 2,4-dichlorophenol over Pd/Al<sub>2</sub>O<sub>3</sub> and Pd/C. *J Catal* 225:510–522
- Yuan G, Keane M (2007) Aqueous-phase hydrodechlorination of 2,4-dichlorophenol over Pd/Al<sub>2</sub>O<sub>3</sub>: reaction under controlled pH. *Ind Eng Chem Res* 46:705–715
- Zhang F, Meng Y, Gu D, Chen Y, Tu B, Zhao D (2006) An aqueous cooperative assembly route to synthesize ordered mesoporous carbons with controlled structures and morphology. *Chemistry* 18:5279–5288
- Zhang F, Jin J, Zhong X, Li S, Niu J, Li R, Ma J (2011) Pd immobilized on amine-functionalized magnetite nanoparticles: a novel and highly active catalyst for hydrogenation and Heck reactions. *Green Chem* 13:1238–1243
- Zhang P, Gong Y, Li H, Chen Z, Wang Y (2013) Solvent-free aerobic oxidation of hydrocarbons and alcohols with Pd@N-doped carbon from glucose. *Nat Commun* 4:1593